



OPEN ACCESS

EDITED BY

Jing-hua Wang,
Daejeon University, Republic of Korea

REVIEWED BY

Scott A. Read,
Western Sydney University, Australia
Karthickeyan Chella Krishnan,
University of Cincinnati, United States

*CORRESPONDENCE

Murali Ganesan
✉ murali.ganesan@unmc.edu

RECEIVED 14 February 2023

ACCEPTED 17 July 2023

PUBLISHED 03 August 2023

CITATION

Bybee G, Moeun Y, Wang W, Kharbanda KK, Poluektova LY, Kidambi S, Osna NA and Ganesan M (2023) Increased liver stiffness promotes hepatitis B progression by impairing innate immunity in CCl4-induced fibrotic HBV⁺ transgenic mice. *Front. Immunol.* 14:1166171. doi: 10.3389/fimmu.2023.1166171

COPYRIGHT

© 2023 Bybee, Moeun, Wang, Kharbanda, Poluektova, Kidambi, Osna and Ganesan. This is an open-access article distributed under the terms of the [Creative Commons Attribution License \(CC BY\)](#). The use, distribution or reproduction in other forums is permitted, provided the original author(s) and the copyright owner(s) are credited and that the original publication in this journal is cited, in accordance with accepted academic practice. No use, distribution or reproduction is permitted which does not comply with these terms.

Increased liver stiffness promotes hepatitis B progression by impairing innate immunity in CCl4-induced fibrotic HBV⁺ transgenic mice

Grace Bybee^{1,2}, Youra Moeun³, Weimin Wang⁴, Kusum K. Kharbanda^{1,2}, Larisa Y. Poluektova⁴, Srivatsan Kidambi³, Natalia A. Osna^{1,2} and Murali Ganesan^{1,2*}

¹Research Service, Veterans Affairs Nebraska-Western Iowa Health Care System, Omaha, NE, United States, ²Department of Internal Medicine, University of Nebraska Medical Center, Omaha, NE, United States, ³Department of Chemical and Biomolecular Engineering, University of Nebraska at Lincoln, Lincoln, NE, United States, ⁴Department of Pharmacology and Experimental Neuroscience, University of Nebraska Medical Center, Omaha, NE, United States

Background: Hepatitis B virus (HBV) infection develops as an acute or chronic liver disease, which progresses from steatosis, hepatitis, and fibrosis to end-stage liver diseases such as cirrhosis and hepatocellular carcinoma (HCC). An increased stromal stiffness accompanies fibrosis in chronic liver diseases and is considered a strong predictor for disease progression. The goal of this study was to establish the mechanisms by which enhanced liver stiffness regulates HBV infectivity in the fibrotic liver tissue.

Methods: For *in vitro* studies, HBV-transfected HepG2.2.15 cells were cultured on polydimethylsiloxane gels coated by polyelectrolyte multilayer films of 2 kPa (soft) or 24 kPa (stiff) rigidity mimicking the stiffness of the healthy or fibrotic liver. For *in vivo* studies, hepatic fibrosis was induced in C57Bl/6 parental and HBV+ transgenic (HBVTg) mice by injecting CCl4 twice a week for 6 weeks.

Results: We found higher levels of HBV markers in stiff gel-attached hepatocytes accompanied by up-regulated OPN content in cell supernatants as well as suppression of anti-viral interferon-stimulated genes (ISGs). This indicates that pre-requisite “fibrotic” stiffness increases osteopontin (OPN) content and releases and suppresses anti-viral innate immunity, causing a subsequent rise in HBV markers expression in hepatocytes. *In vitro* results were corroborated by data from HBVTg mice administered CCl4 (HBVTg CCl4). These mice showed higher HBV RNA, DNA, HBV core antigen (HBcAg), and HBV surface antigen (HBsAg) levels after liver fibrosis induction as judged by a rise in Col1a1, SMA, MMPs, and TIMPs mRNAs and by increased liver stiffness. Importantly, CCl4-induced the pro-fibrotic activation of liver cells, and liver stiffness was higher in HBVTg mice compared with control mice. Elevation of HBV markers and OPN levels corresponded to decreased ISG activation in HBVTg CCl4 mice vs HBVTg control mice.

Conclusion: Based on our data, we conclude that liver stiffness enhances OPN levels to limit anti-viral ISG activation in hepatocytes and promote an increase in HBV infectivity, thereby contributing to end-stage liver disease progression.

KEYWORDS

HBV, liver stiffness, innate immunity, alcohol, osteopontin (OPN)

Introduction

In approximately 10% of cases, Hepatitis B virus (HBV) infection becomes chronic and progresses from steatosis, hepatitis, and fibrosis to end-stage liver diseases such as cirrhosis and hepatocellular carcinoma (HCC). Approximately 400 million individuals worldwide have chronic hepatitis B (CHB) and almost one million die annually from complications due to persistent infection, liver cirrhosis, and HCC. (1–5) Despite the availability of an efficient vaccine, chronic HBV infection persists. (6) In adults, horizontal transmission mainly results in self-limiting acute HBV infection, while vertical transmission leads to CHB. (7) Current treatments include interferon-based therapies and several nucleos(t)ide analogs. While nucleos(t)ide analogs rarely cure CHB, they suppress viral replication which slows down disease progression that would otherwise eventually manifest as end-stage liver disease. (8) HBV is still the most frequent cause of liver fibrosis (9), so current treatment strategies are focused on the long-term suppression of HBV replication. Hepatic stellate cells (HSCs) activation is a crucial pathogenic feature of liver fibrosis that makes it a hotspot in this research field. HBV triggers HSCs activation via DAMPs release and the host antiviral immune response, leading to chronic inflammation. (10) However, unlike the hepatitis C virus (HCV), the mechanisms of liver fibrosis development remain less defined in CHB.

HBV is not cytotoxic, and the infected hepatocytes are eliminated by immune mechanisms. The first line of anti-viral defense, which secures the effective adaptive immune response, is related to innate immunity, specifically to the activation of anti-viral interferon-stimulated genes (ISGs) to resist/control HBV infection

in hepatocytes, thereby preventing its spread and persistence. HBV infects only hepatocytes, which are removed by the immune system, causing continuous cycles of hepatocyte damage followed by tissue repair. This requires the deposition of the extracellular matrix with subsequent progressive liver fibrosis over time. (11, 12) An increased stromal stiffness accompanies fibrosis in chronic liver diseases (13) and serves as a strong predictor of disease progression to end-stage liver diseases (14), including hepatitis B. (15) Clinically viewed as the indicator of organ fibrosis, tissue stiffness increases remarkably in line with deposition, cross-linking, and reconstruction of the matrix. (16) Recent studies have shown that matrix stiffness plays a pivotal role in fibroblast activation and outcomes of pathological fibrosis. (16, 17)

It has been suggested that matrix stiffness plays a role in the regulation of some biochemical markers expression, such as osteopontin (OPN). (18, 19) OPN is a matricellular glycoprophosphoprotein produced by different cells and is associated with the synthesis and accumulation of the extracellular matrix (ECM) and, therefore, promotes fibrosis progression. (20) Importantly, serum osteopontin (OPN) concentrations were found to be significantly increased in HBV-infected patients and patients with hepatocellular carcinoma (HCC). (21) In addition, the role of OPN has been elucidated in inflammatory liver disorders, such as T cell-mediated hepatitis and alcoholic and nonalcoholic disorders. (22–24) However, to date, there are no thorough investigations on liver stiffness, the role of OPN expression, and HBV infection pathogenesis. The aim of this study was to establish the mechanisms by which enhanced liver stiffness regulates HBV infection levels in liver fibrosis.

In this study, we aimed to analyze both *in vitro* and *in vivo* evidence of a liver stiffness-mediated increase of HBV markers in HBV-transfected HepG2.2.15 cells and in HBV-infected fibrotic liver. We hypothesize that a pre-requisite “fibrotic” stiffness increases OPN levels in hepatocytes and suppresses anti-viral innate immunity, causing a subsequent rise in the expression of HBV markers. For *in vitro* studies, HBV-transfected HepG2.2.15 cells were cultured on an innovative biomimetic platform named BEASTS (Bio-Engineered Adhesive Siloxane substrate with Tunable Stiffness) that utilizes a polydimethylsiloxane (PDMS) substrate, along with polyelectrolyte multilayer film-coating technology. By employing this approach, we can engineer substrates that closely mimic physiological (2 kPa) and fibrotic (24 kPa) stiffnesses of the liver (25–29). *In vitro* results were confirmed by *in vivo* studies, in

Abbreviations: α -SMA, α -Smooth Muscle Actin; ALT, Alanine Aminotransferase; AST, Aspartate Aminotransferase; CCl₄, Carbon tetrachloride; CHB, Chronic HBV; CLD, Chronic Liver Diseases; ddPCR, Digital Droplet PCR; ECM, Extracellular Matrix; HBcAg, hepatitis B core antigen; HBsAg, HBV Surface Antigen; HBVTg, HBV+ Transgenic mice; HSCs, Hepatic Stellate Cells; HBV, Hepatitis B Virus; HCV, Hepatitis C Virus; HCC, Hepatocellular Carcinoma; IFN α , Interferon α ; ISGs, Interferon-Stimulated Genes; OPN, Osteopontin; PDAC, Poly (diallyldimethylammonium) Chloride; PDMS, Polydimethylsiloxane; PEMs, Polyelectrolyte Multilayer films; RT-PCR, Real-time PCR; rOPN, Recombinant Human Osteopontin; SPS, Sulfonated Poly(styrene) Sodium salt; TIMPs, Tissue Inhibitors of Matrix Metalloproteinases.

which hepatic fibrosis was induced in C57Bl/6 parental and HBV⁺ transgenic (HBVTg) mice by injecting CCl₄ twice a week for 6 weeks to mimic fibrotic liver. This current study will help in identifying the mechanisms by which liver tissue stiffness regulates the pathogenesis of HBV infection allowing for the detection of new targets for treatment.

Materials and methods

Reagents and media

High glucose Dulbecco's Modified Eagle Medium (DMEM) and fetal bovine serum were purchased from Invitrogen (Carlsbad, CA). Trizol was acquired from Life Technologies (Carlsbad, CA). All RNA isolation, cDNA synthesis, and RT-PCR reagents and primers (human and mouse) were obtained from ThermoFisher Scientific (Carlsbad and Foster City, CA). The DNA isolation kit was obtained from Qiagen (Louisville, KY). Human Osteopontin DuoSet and Mouse Osteopontin DuoSet ELISA kits were obtained from R&D Systems (Minneapolis, MN). Interferon α (IFN α) was purchased from Merck Sharp & Dohme Corp (NJ, USA; cat# NDC 0085-0571-02). We used the following antibodies: anti-Hepatitis B core antigen and anti-Hepatitis B surface antigen from INNOVEX Biosciences Inc (Richmond, CA), α SMA from Abcam (Cambridge, MA), anti-pSTAT-1, cleaved caspase 3 and anti-USP18 from Cell Signaling Technology (Beverly, MA), and anti-STAT-1 and Anti- β actin from Santa Cruz Biotechnology Inc. (Santa Cruz, CA).

Cell culture and treatments

In this study, we used HepG2.2.15 cells that were stably transfected with HBV and were able to replicate the virus and produce viral particles (HBV genotype D). (30) HepG2.2.15 cells were cultured on an innovative biomimetic platform named BEASTS (Bio-Engineered Adhesive Siloxane substrate with Tunable Stiffness) based on polydimethylsiloxane (PDMS) substrate in combination with polyelectrolyte multilayer film-coating technology to engineer substrates mimicking physiologic (2 kPa) and fibrotic liver stiffness (24 kPa). (25–29) In summary, Sylgard 527 and Sylgard 184 were mixed in specific weight ratios, as outlined in Table 1, and crosslinked according to the manufacturer's instructions. For Sylgard 527, components A and B were mixed in equal parts, while Sylgard 184 was mixed in a ratio of 10:1 of elastomer to the cross-linking agent. The two mixtures were

TABLE 1 Young's Modulus of PEM-coated PDMS substrates used for primary hepatocyte culture was determined using the indentation load technique.

Substrate	Young's Modulus (in KPa)
Soft (100% Sylgard 527)	2.4 ± 0.03
Stiff (91% wt Sylgard 527 + 9% wt Sylgard 184)	24.2 ± 0.03

then combined in a determined weight ratio and poured into 12-well tissue culture plates to crosslink at 65 °C. The resulting PDMS gels were then rendered hydrophilic through a 7-minute oxygen plasma treatment before being coated with PEMs using poly (diallyldimethylammoniumchloride) (PDAC) (Mw~100,000-200,000) as a 20 wt % solution, and sulfonated poly(styrene) and sodium salt (SPS) (Mw~70,000) polymer solutions. This was achieved by immersing the PDMS substrates in alternating polycation and polyanion solutions to form multiple layers and was repeated five times. The resulting platform was then UV-sterilized overnight before being used to study the effects of stiffness on HBV-infected hepatocytes in a non-invasive environment. To study the type-1 IFN α signaling, cells were treated or not with interferon-alpha (IFN α) for 8hrs at 400 units concentration.

Recombinant osteopontin treatment

To mimic the overexpression of osteopontin, we used recombinant human osteopontin (rOPN) Protein from R & D Systems, Catalog #: 1433-OP. We pre-treated the cells in the presence or absence of rOPN at 100 nM for 24hrs, and IFN α was applied for the last 8 hours (400 units) to induce the IFN α signaling.

Osteopontin siRNA transfection

Transfection was done using the protocol from the manufacturer (OriGene, Rockville, MD) with control (scrambled) or osteopontin siRNA (Cat#SR321880 SPP1). The efficacy of transfection was monitored for 48hrs for the osteopontin mRNA expression by RT-PCR. Human OPN Primer (Hs00959010_m1) was gotten from Thermo Fisher, Catalog #: 4331182.

RNA and DNA isolation, real-time PCR, and ddPCR

Total RNA was isolated from cells using Trizol Reagent. DNA was isolated from cells using DNeasy Blood and Tissue kit (Qiagen, Louisville, KY) following the manufacturer's instructions. RT-PCR was used to measure HBV RNA, OAS1, ISG15, APOBEC3G, USP18, Col1A1, TGF β 1, α -SMA, MMP2, and MMP9 mRNA levels in cells as described previously (31). ddPCR was used to quantify HBV DNA levels in HepG2.2.15 cells as previously described (32) using the following primers and probes: HBV sense (5'- CGA CGT GCA GAG GTG AAG-3'), antisense (5'- CAC CTC TCT TTA CGC GGA CT-3') primers, and HBV probe (5'-/56-FAM/ATC TGC CGG/ZEN/ ACC GTG TGC AC/3IABkFQ/-3').

ELISA

HBV surface antigen (HBsAg) and human osteopontin were measured in cell media by ELISA using LSBio Kit (LifeSpan

Biosciences, Inc, Seattle, WA) and DuoSet Kit (R&D Systems, Minneapolis, MN), respectively.

Immunoblotting (western blot)

Cell lysates prepared in 0.5 M EDTA, 2 M Tris, 20 mM Na₃VO₄, 200 mM Na₄P₂O₇, 100 mM PMSF, 1 M NaF, 20% Triton X-100, and aprotinin, pH 7 were separated and subjected to the immunoblotting technique as previously described (32, 33). Blots were developed using the Odyssey infrared imaging system, and the protein bands were quantified using the Li-Cor software (Li-Cor Bioscience, Lincoln, NE).

In vivo studies

Experimental manipulations on HBV+ transgenic mice

HBV+ transgenic (HBVTg) mice are a specially designed strain that carry the 1.3mer, over-length wild-type HBV genome, which expresses all viral proteins except the X protein. These mice were obtained from Dr. Jing-Hsiung James Ou, Professor of Molecular Microbiology and Immunology, University of Southern California, Los Angeles (MTA on 04/21/2021). The DNA fragment used for producing the transgenic mice starts from nucleotide (nt) 1043, which is located upstream of the ENI enhancer and the X promoter, and terminates at nt 1987 located downstream of the unique poly (A) site. Sixteen mice were split equally into four groups (four mice per group): control C57Bl/6 (HBV-), C57Bl/6 with induced hepatic fibrosis (CCl₄), control HBVTg (HBV+), and HBVTg with induced hepatic fibrosis (HBV+CCl₄). All animals received humane care, and all methods were carried out in accordance with the Guide for the Care and Use of Laboratory Animals and were approved by the Institutional Animal Care and Use Committee. Hepatic fibrosis was induced in male and female C57BL/6J and HBVTg (HBV+) mice using CCl₄ as described (34, 35). Briefly, CCl₄ was diluted 1:7 in sunflower oil and injected intraperitoneally (i.p.) twice per week at a dose of 1 µl/g body weight (0.125 µl/g CCl₄) for 6 weeks (35).

Serum enzyme measurements

The clinical laboratory at the VA NWIHCS analyzed the activity of alanine aminotransferase (ALT) and aspartate aminotransferase (AST).

RNA and DNA isolation, Real-time PCR, and ddPCR

Total RNA was isolated from mouse liver tissue using Trizol Reagent; DNA was isolated using DNeasy Blood and Tissue kit (Qiagen, Louisville, KY) following the manufacturer's instructions. RT-PCR was used to measure HBV RNA, Col1a1, α-SMA, TIMP1, TIMP2, MMP2, MMP9, MMP13, and OPN mRNA levels in liver tissue as described previously (33). ddPCR was applied to quantify HBV DNA levels as previously described (33) using the following primers and probes: HBV sense (5'- CGA CGT GCA GAG GTG

AAG-3'), antisense (5'- CAC CTC TCT TTA CGC GGA CT-3') primers, and HBV probe (5'-/56-FAM/ATC TGC CGG/ZEN/ACC GTG TGC AC/3IABkFQ/-3').

Histology and immunohistochemistry

To visualize collagen accumulation, sections of paraffin-embedded liver tissue were subjected to picrosirius red staining (36). For the immunohistochemical detection of α-smooth muscle actin (α-SMA), HBcAg, and HBsAg, sections were heated in antigen unmasking solution (Vector Labs, Burlingame, CA, USA), then probed with respective antibodies, and visualized using a Keyence BZ-X810 fluorescence microscope. Staining intensity in the captured images was quantified using the Keyence BZ-X810 Analyzer software. At least, 10 non-overlapping fields per low magnification (20X) section were analyzed.

ELISA

Mouse osteopontin DuoSet Kit (R&D Systems, Minneapolis, MN) was used to measure osteopontin levels in the media and serum.

Mechanical analysis of liver tissue

To determine the compressive Young's modulus of the liver tissue, a microscale mechanical testing apparatus called the CellScale BioTester (Waterloo, Canada) was used. The samples were equilibrated at 37 °C and preconditioned for two cycles at 0.8 µm/s strain rate to eliminate hysteresis effects before each measurement. Compression was then performed at 10% strain with 30 s compression followed by a 2-second hold and 10-second recovery. The force versus displacement curve was analyzed using a custom MATLAB code to calculate Young's modulus by measuring the slope of the curve.

Statistical analyses

The data were expressed as mean values ± standard error. A one-way analysis of variance (ANOVA) was performed on the multiple groups of this study and a comparison was made using a Tukey *post-hoc* test. A Student's t-test was used to compare two groups at a time. Results were considered significant at a probability value of 0.05 or less.

Results

Increased matrix stiffness upregulates HBV infection markers and OPN levels in HBV-transfected HepG2.2.15 cells

To investigate the role of increased matrix stiffness in the regulation of HBV expression in HepG2.2.15 cells, we quantified HBV RNA and DNA by RT-PCR and ddPCR, respectively, and used ELISA to quantify HBsAg levels (Figures 1A-C). We found that plating the cells at the increased matrix stiffness upregulated HBV markers by approximately 2.5-fold as evident from the results of stiff

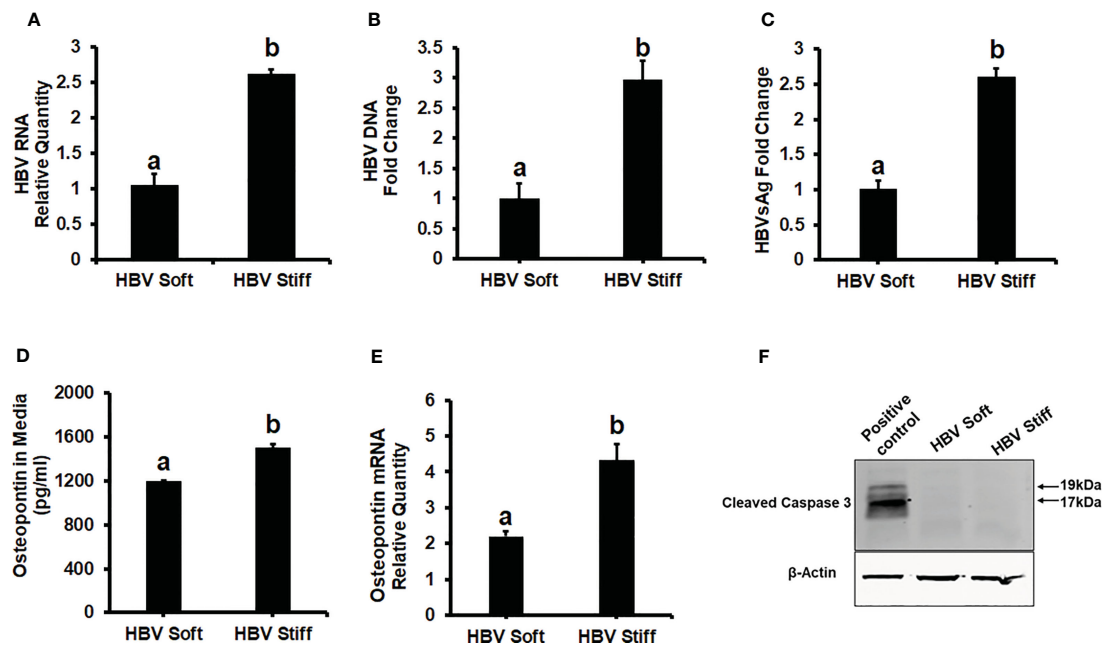


FIGURE 1

Increased matrix stiffness upregulates HBV infection markers and osteopontin levels in HBV-transfected HepG2.2.15 cells: Cells were plated in both soft and stiff plates for 48hrs. (A) HBV RNA levels were measured by Real-Time PCR. (B) HBV DNA levels were measured by Droplet Digital™ PCR (ddPCR). GAPDH was used as an internal control for HBV RNA and HBV DNA. (C) A Sandwich Elisa kit was used to measure HBsAg levels. (D, E) Osteopontin protein and mRNA levels were measured by Elisa and Real-Time PCR. (F) Cleaved caspase 3 protein expression was detected by immunoblotting in cell lysates for apoptosis. Equal (20 ug) amounts of protein were loaded in each lane. β -Actin was used as an internal control. Acetaldehyde-generating system (AGS)-treated HepG2 cell lysates were used as the positive control. Data are from three independent experiments presented as Mean \pm SEM. Bars marked with the same letter are not significantly different from each other; bars with different letters are significantly different ($p \leq 0.05$).

gel- (25 kPa) vs soft gel-attached cells. Enhanced matrix stiffness also increased OPN expression in these cells, and there is a correlation between osteopontin (OPN) levels and the expression of HBV markers. We measured OPN protein levels in the cell media and mRNA expression in cells and observed that higher levels of HBV markers in fibrotic stiff gel-attached hepatocytes were accompanied by up-regulated OPN protein content ($p < 0.05$) in cell supernatants as well as OPN mRNA expression in cells (Figures 1D, E). In addition, we confirmed that there was no apoptotic cell death in fibrotic stiffness gel-attached HepG2.2.15 cells (Figure 1F).

Increased matrix stiffness suppresses IFN α signaling in HBV-transfected HepG2.2.15 cells

Next, we tested whether the up-regulation of HBV infection markers was related to suppressed anti-viral interferon-stimulated genes and the impairment of IFN α -signaling via the JAK-STAT1 pathway. In this regard, in healthy (2 kPa) and fibrotic stiffness (25 kPa) gel-attached HepG2.2.15 cells, we measured mRNA expression of ISGs (*OAS1*, *ISG15*, and *APOBEC3G*) as well as STAT1 phosphorylation (Immunoblotting) in response to IFN α . We found that fibrotic stiffness gel-attached cells show a significant decrease ($p < 0.05$) in ISGs mRNA expression (Figures 2A–C) and also a 2-fold reduction in the pSTAT1/STAT1 ratio (Figures 2D, E), when compared to the healthy stiffness gel-attached HBV-expressing

cells, suggesting that fibrotic stiffness suppresses downstream events of IFN α signaling. In addition to this, we also found that both mRNA (Figure 2G) and protein expression (Figures 2D, F) of USP18, a negative regulator of IFN signaling, were significantly increased in fibrotic stiffness gel-attached HepG2.2.15 cells when compared to healthy stiffness gel-attached cells.

OPN increases the expression of HBV markers by suppressing IFN α -inducible anti-viral genes activation in soft gel-attached HBV+ transfected HepG2.2.15 cells

To prove that OPN downregulates ISGs, we treated soft (2 kPa) gel-attached HBV-transfected HepG2.2.15 cells with rOPN (to mimic overexpression). The rOPN treatment of soft gel-attached HepG2.2.15 cells successfully impaired the IFN α signaling by suppressing the mRNA expression of ISGs, *OAS1*, *APOBEC3G*, and *ISG15* as well as the protein expression of pSTAT-1 in response to IFN α , resulting in increased HBV RNA levels when compared to soft gel-attached cells not exposed to OPN (Figures 3A–F). This experiment (Figure 3) was performed on soft gels since OPN expression is higher in stiff gel vs soft gel. Thus, we tried to mimic OPN levels in the cells plated on stiff gels by overexpressing OPN (treatment with recombinant OPN) in cells plated on soft gels and then measured ISG expressions. In addition, we silenced OPN by specific siRNA transfection, (to mimic knock-down)

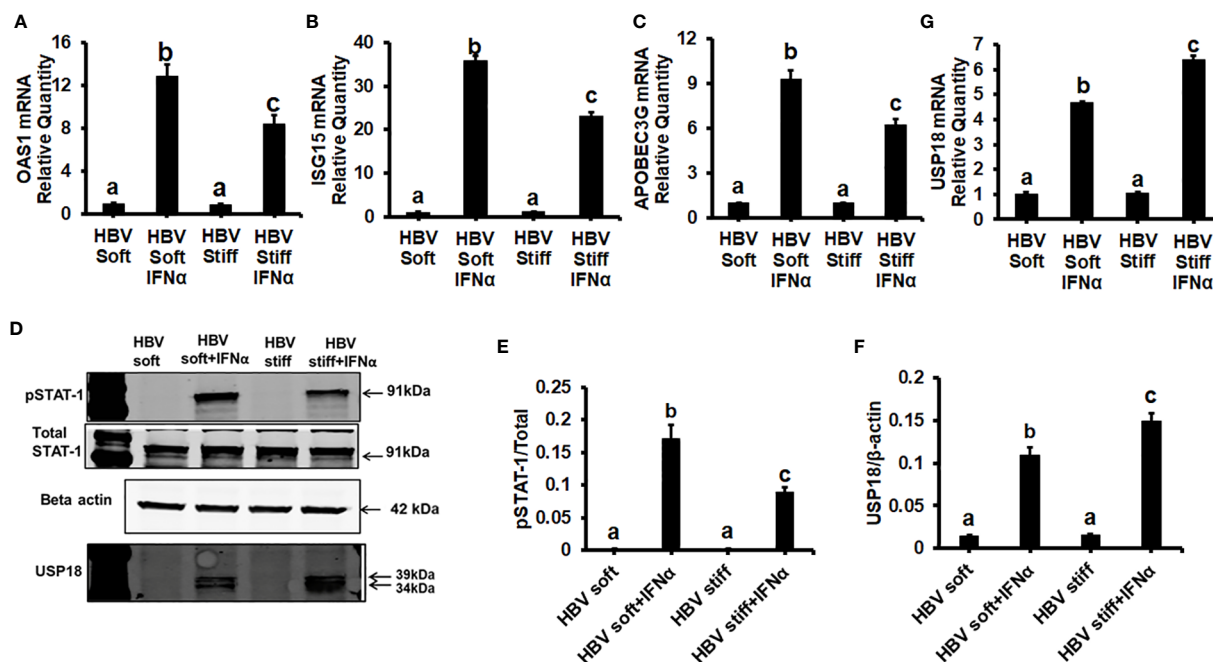


FIGURE 2

Increased matrix stiffness suppresses IFN α signaling in HBV transfected HepG2.2.15 cells: HepG2.2.15 cells were either treated or not treated with IFN α for the last 8 hours (ISGs), 1 hr (pSTAT-1), and 24 hours (USP18 protein). RT-PCR analysis was done for mRNA expression of IFN-induced genes. (A) 2'-5' oligoadenylate synthetase 1 (OAS1); (B) Interferon-stimulated gene 15 (ISG15); (C) Apolipoprotein B Editing Complex (APOBEC3); (G) USP18. GAPDH acted as an internal control. (D) STAT-1 phosphorylation (pSTAT-1) and USP18 protein were measured by immunoblotting. Total STAT-1 was used to normalize the data and β -actin was also used as an internal control. (E, F) Quantification of immunoblotting data. Data are from three independent experiments presented as Mean \pm SEM. Bars marked with the same letter are not significantly different from each other; bars with different letters are significantly different ($P \leq 0.05$).

in soft (2 kPa) and stiff (25 kPa) gel-attached HBV-transfected HepG2.2.15 cells. Silencing OPN (Figure 4A) enhanced anti-viral gene activation with reduced HBV RNA levels. IFN α significantly suppressed the HBV RNA levels (Figures 4B-E).

Possible mechanisms of the regulation of HBV infection markers by OPN in fibrotic stiffness gel-attached HBV+ transfected HepG2.2.15 cells

To investigate how OPN regulates the levels of HBV infection markers in fibrotic stiffness (25 kPa) gel-attached HBV-transfected cells, we measured the *USP18* mRNA expression (a negative regulator of IFN signaling) in the presence of IFN α either in OPN-silenced soft (2 kPa) and stiff (25 kPa) gel-attached HepG2.2.15 cells or in rOPN-treated soft (2 kPa) gel-attached HepG2.2.15 cells. We observed that OPN silencing significantly ($p < 0.05$) decreased *USP18* mRNA levels (Figure 4F) in fibrotic stiffness gel-attached HepG2.2.15 cells, whereas rOPN treatment did not increase the *USP18* mRNA expression in soft gel-attached HepG2.2.15 cells when compared to IFN α -treated group (Figure 4G). We performed this experiment (4G) on soft gels. Since we found that OPN expression was higher on stiff gel vs soft gel, we tried to mimic this by overexpressing OPN (treatment with recombinant OPN) in cells plated on the soft gel. In addition, we observed that recombinant OPN treatment significantly increased

the *USP18* protein expression in soft gel attached HepG2.2.15 cells when compared to control cells (Figure 4H).

In vivo evidence of the role of liver tissue stiffness in HBV infection pathogenesis

To confirm our *in vitro* findings that an increased matrix stiffness regulates HBV-replication/enhanced expression of HBV markers, liver fibrosis was induced by injecting CCl₄ for 6 weeks in C57Bl/6 parental and HBV+ transgenic (HBVTg) mice. Liver tissue stiffness was measured using the Biotester (CellScale Biomaterial Testing). We observed that the liver stiffness was higher (2-fold) in CCl₄-administered HBVTg mice as well as in wild-type mice compared with control mice of each group (Figure 5A). As shown in Figure 5A, the *ex vivo* liver tissue stiffness of control mice reads 17 kPa. This is due to possible alterations in mechanical properties in *ex vivo* tissues due to perfusion pressure, tissue degradation, and boundary condition compared to *in vivo* environment. Also, this study indicates that the mechanical properties change drastically within only several minutes postmortem. (37) To account for this deviation, we processed all the conditions on the same day to measure the stiffness and the comparison in stiffness to indicate the changes in the original stiffness under each treatment condition. Based on the above-mentioned changes, the liver tissue stiffness in wild-type control mice is considered to represent the stiffness in the healthy liver, while the CCl₄-induced increase in liver stiffness corresponds to fibrotic

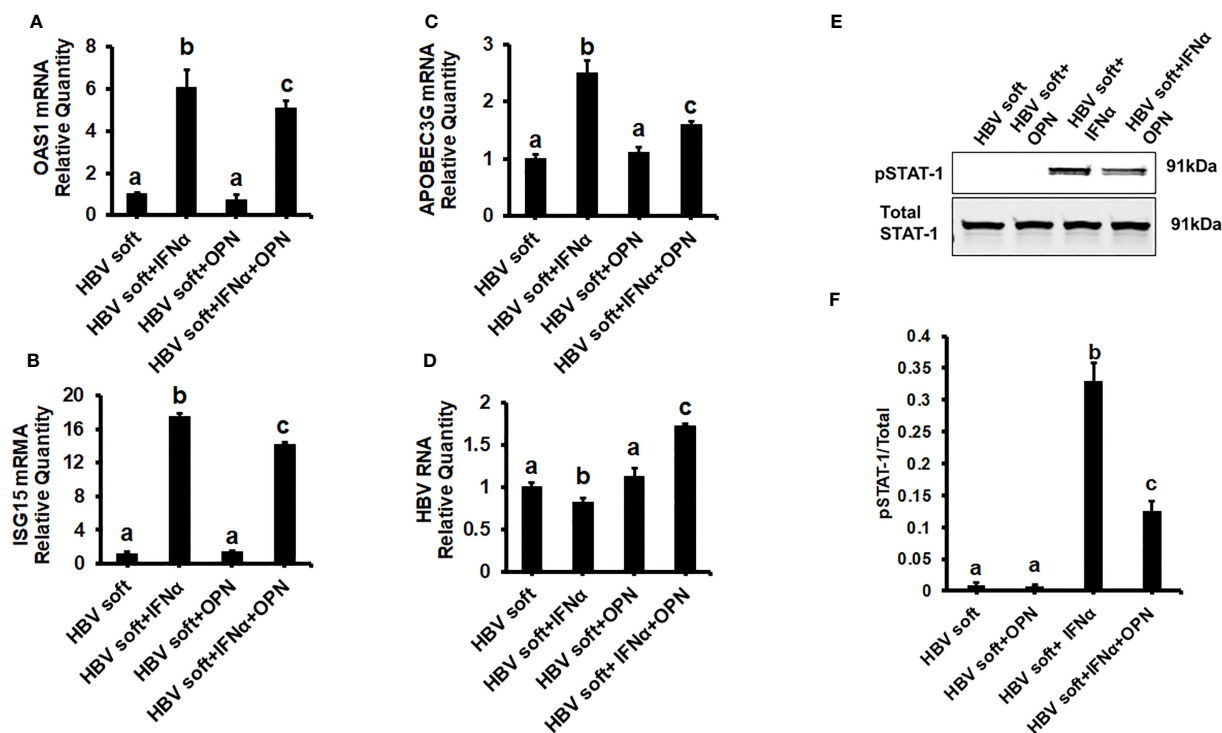


FIGURE 3

Recombinant OPN treatment increases the expression of HBV marker by suppressing IFN α -inducible anti-viral genes activation in soft gel (2 kPa) attached HBV+ transfected HepG2.2.15 cells: To mimic overexpression, we treated soft (2 kPa) gel-attached HBV transfected HepG2.2.15 cells with rOPN for 24hrs. RT-PCR analysis was done for mRNA expression of IFN-induced genes and HBV RNA. (A) 2'-5' oligoadenylate synthetase 1 (OAS1); (B) Interferon-stimulated gene 15 (ISG15); (C) Apolipoprotein B Editing Complex (APOBEC3); (D) HBV RNA. GAPDH acted as an internal control. (E) STAT-1 phosphorylation (pSTAT-1) was measured by immunoblotting. Total STAT-1 was used to normalize the data. (F) Quantification of immunoblotting data. Data are from three independent experiments presented as Mean \pm SEM. Bars marked with the same letter are not significantly different from each other; bars with different letters are significantly different ($P \leq 0.05$).

stiffness. Interestingly, control HBVTg mice showed higher liver tissue stiffness when compared to control wild-type mice. To determine whether the observed increased liver tissue stiffness plays a role in the up-regulation of HBV infection markers in CCl₄-administered HBVTg mice, we measured HBV RNA and DNA in mouse livers and HBV DNA levels in serum by COBAS Amplicor HBV monitor test and performed immunohistochemical analysis of HBcAg and HBsAg in the liver (Figures 5B-H). These HBV-specific markers were significantly elevated ($p \leq 0.05$) in the livers of CCl₄-administered HBVTg mice. In addition, we found that both mRNA and protein expressions of OPN were significantly increased in the livers and serum of CCl₄-administered control and HBVTg mice when compared to the respective control wild-type and control HBVTg mice (Figures 6A, B).

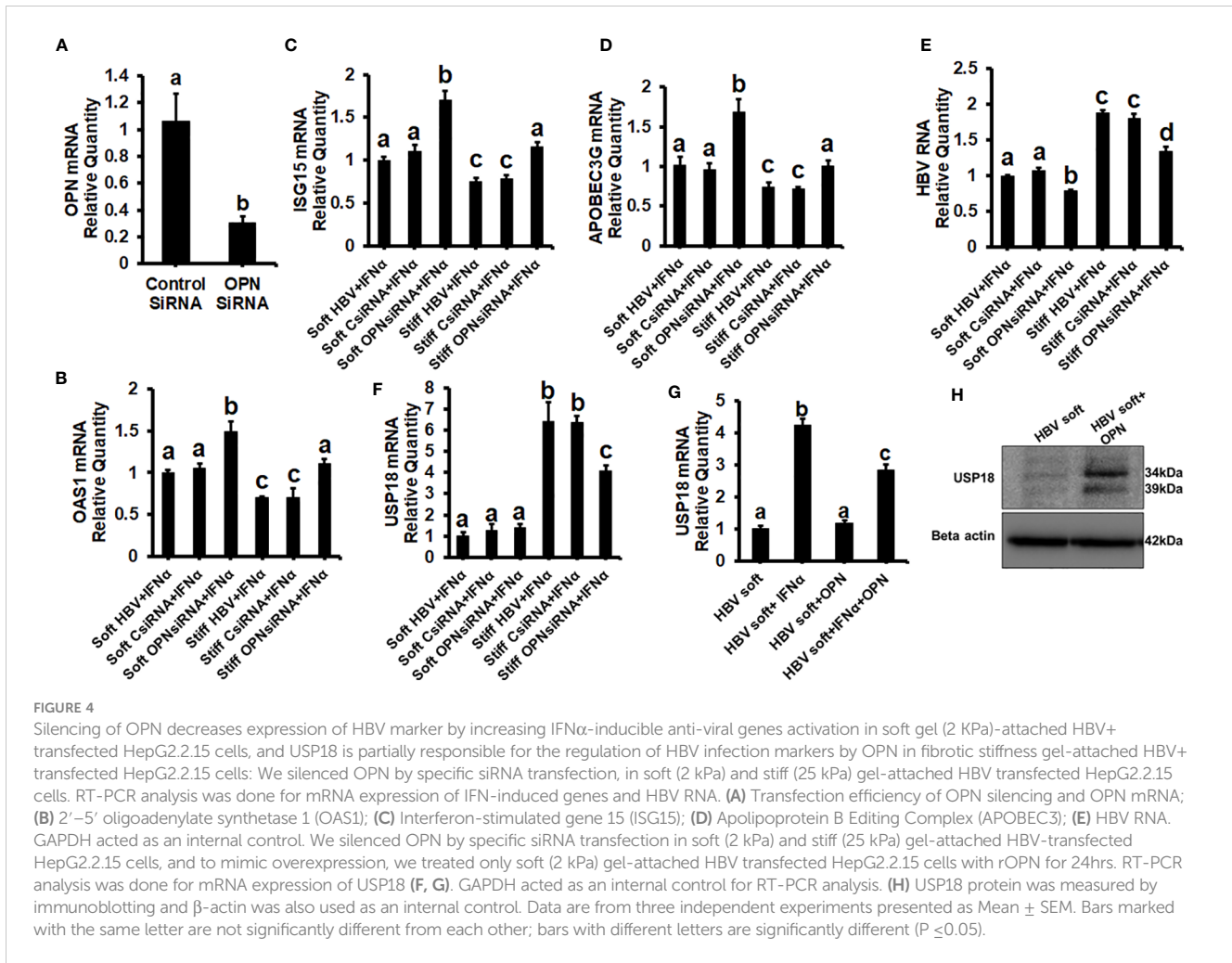
Liver tissue stiffness suppresses ISGs expression in the livers of CCl₄-administered HBVTg mice

Since in our *in vitro* study we found that increased stiffness induced up-regulation of OPN and regulates HBV-infection markers due to the suppression of IFN α -inducible anti-viral genes, we wanted to check whether an increase in liver tissue stiffness exerts the same

effect in CCl₄-administered HBVTg mice. To this end, we measured the mRNA expression of ISGs, OAS1, ISG15, and APOBEC. These mRNA expressions were significantly ($P < 0.05$) decreased in the livers of CCl₄-administered HBVTg mice when compared to control HBVTg mice (Figures 6C-E). We also found that the mRNA expression level of the negative regulator of IFN α signaling, *USP18*, was increased both in the CCl₄-administered wild type and HBVTg mice (Figure 6F). There was no alteration in the mRNA expression of ISGs in CCl₄-administered wild-type mice when compared to control wild-type mice.

CCl₄ induces hepatic fibrosis in HBV- and HBV+ transgenic mice

The livers were analyzed by picrosirius staining and immunohistochemical analysis to identify the collagen content and α -smooth muscle actin (SMA) (Figures 7A-D). The mice receiving CCl₄ had a 2-fold increase in collagen and SMA expression when compared to control (unmanipulated) mice, which confirmed that fibrosis had been established. In addition, there was an increase in ALT and AST levels in CCl₄-treated mice when compared to control mice (Figures 7E, F). HBVTg control mice showed elevated AST levels when compared to control wild-type mice. Total body and liver weights were



not significantly different between the groups (Data not shown). The rate of collagen I gene (*Col1A1*) and *SMA* expression was determined using RT-PCR. A significant increase ($p \leq 0.05$) in *Col1A1* and *SMA* expression was established by CCL4 treatment in wild-type and HBVTg mice (Figures 8A, B). Proteolysis is a major mechanism in the regulation of collagen levels. MMPs degrade collagen and other extracellular matrix proteins and are also regulated by their endogenous inhibitors and tissue inhibitors of matrix metalloproteinases (TIMPs). We found that expression of MMPs (MMP2, 9, and 13) and TIMPs (TIMP1 and 2) were significantly increased ($p \leq 0.05$) in CCL4-exposed wild-type and HBVTg mice when compared to control mice of these types (Figures 8C-G).

Discussion

Though adaptive immune response by HBV-specific CD8+ T cell (cytotoxic T-lymphocytes-CTLs) is largely responsible for clearing HBV-infected hepatocytes and disease pathogenesis (38), we cannot ignore the host's first line of defense, the innate immune response. (39, 40) During HBV infection, antiviral innate immunity is activated when host-pathogen recognition receptors (PRRs) recognize the pathogen-associated molecular patterns (PAMPs) of the virus. (41, 42) The liver

is an important immune organ, enriched with innate immune cells mounting a rapid and robust immune response. (43, 44) Hepatocytes are responsible for the biosynthesis of 80–90% of innate immune proteins. (45, 46) Furthermore, dysfunctional immune responses play an essential role in liver inflammation and persistent HBV infection. (4, 47–49) The increase in liver stiffness is driven by the inflammatory process, significantly pronounced CHB, (50), and correlates with liver decompensation, development of hepatocellular carcinoma, and patient survival. Thus, the measurement of liver stiffness is a non-invasive tool for monitoring CHB progression (51) to determine liver fibrosis and evaluate the efficiency of the treatment. (52) In this study, we aimed to investigate the role of increased liver stiffness in HBV infection pathogenesis addressed by both *in vitro* and *in vivo* experiments. Here, we hypothesized that matrix stiffness enhances OPN levels to limit anti-viral ISG activation and promote the increase in HBV infectivity, thereby contributing to end-stage liver disease progression.

For *in vitro* studies, an innovative biomimetic platform called BEASTS (Bio-Engineered Adhesive Siloxane substrate with Tunable Stiffness) was developed by combining a polydimethylsiloxane (PDMS) substrate with polyelectrolyte multilayer film-coating technology. This enabled us to engineer substrates that mimic both physiologic (2 kPa) and fibrotic liver stiffness (25 kPa) on which we

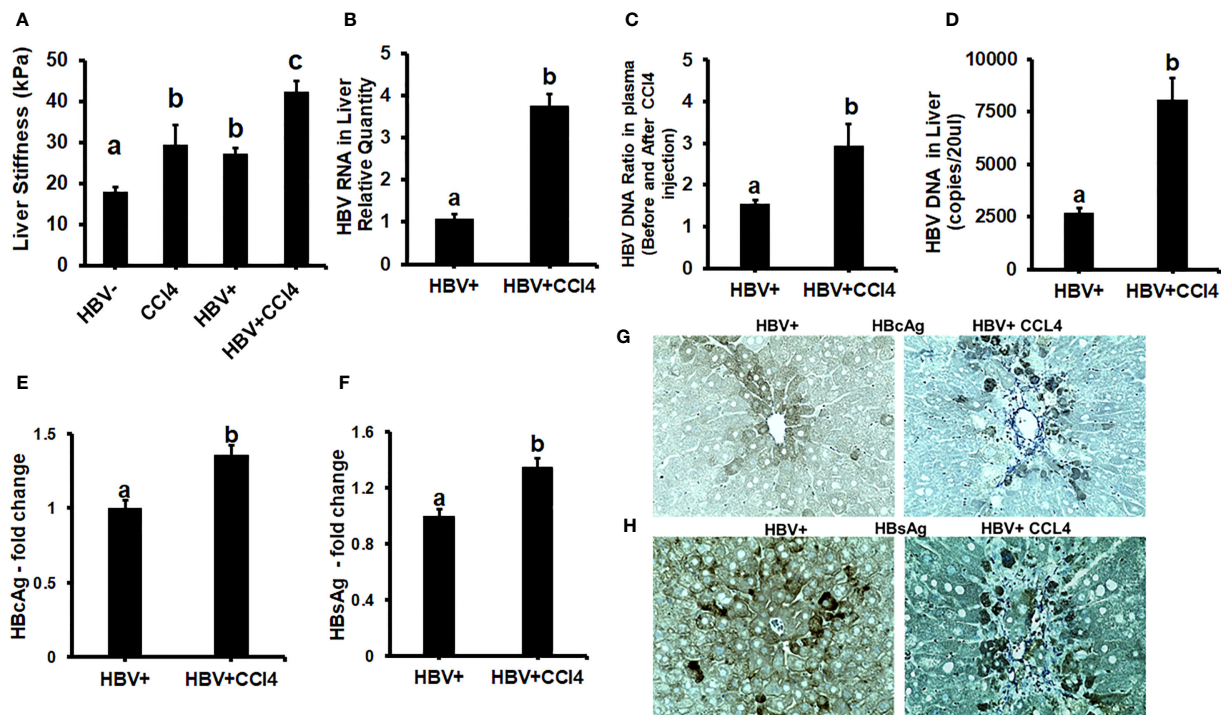


FIGURE 5

Increased liver tissue stiffness regulates HBV replication/enhanced expression of HBV markers in livers of CCl4-administered HBV+ transgenic mice (HBVTg): (A) Liver tissue stiffness was measured using the Biotester (CellScale Biomaterial Testing); (B) HBV RNA levels were measured by Real-Time PCR; (C) HBV DNA levels in serum by COBAS Amplicor HBV monitor test; (D) HBV DNA levels in the liver was measured by ddPCR; (E-H) Immunohistochemical detection of HBcAg, and HBsAg was visualized using a Keyence BZ-X810 fluorescence microscope. Staining intensity in the captured images was quantified using the Keyence BZ-X810 Analyzer software. At least, 10 nonoverlapping fields per low magnification (20X) section were analyzed. GAPDH was used as an internal control for HBV RNA and HBV DNA. Data are given as Mean \pm SEM (n = 4). The data bars marked with the same alphabetical letter are considered not significantly different, while those marked with differing alphabetical letters are considered significantly different from each other ($p \leq 0.05$).

cultured HepG2.2.15 cells to study their behavior under these two conditions. We found that with increasing matrix stiffness, there was upregulation of HBV markers and OPN levels. This might be due to the ability of OPN to suppress innate immunity that controls viral replication in HBV-transfected HepG2.2.15 cells. One of the most potent mechanisms of anti-viral defense is the induction of ISGs in hepatocytes activated by IFN α via the JAK-STAT1-2 pathways. Therefore, we tested IFN α signaling via the JAK-STAT1 pathway in cells plated on healthy and fibrotic stiffness gels. We found that both upstream STAT1 phosphorylation and downstream activation of ISGs, namely, OAS1, ISG15, and APOBEC3G, were impaired in fibrotic stiffness gel-attached HBV-transfected HepG2.2.15 cells. In addition, we observed that USP18, a negative regulator of IFN signaling, was significantly increased at both the mRNA and protein levels in fibrotic stiffness gel-attached HBV-transfected cells. Importantly, overexpression of OPN (exposure of cells to rOPN) suppressed ISGs and increased HBV RNA levels. In addition, OPN silencing by specific siRNA transfection increased ISG expression and decreased the HBV RNA levels in fibrotic stiffness gel-attached, IFN α -treated, HBV-transfected cells, suggesting that OPN plays a partial role in impairing innate immune response via ISGs suppression. Thus, when cells are under fibrotic stiffness conditions (attached to stiff gels), this leads to an increase in HBV RNA levels.

Our findings were supported by other studies showing that higher matrix stiffness upregulates OPN expression in HCC cells.

(19) In addition, OPN concentrations were increased in CHB patients (53), and OPN was identified as a biomarker of liver fibrosis in hepatitis B. (54) The suppression of STAT1 phosphorylation by increased OPN found in our study is not unique to only chronic HBV infection. In fact, similar to our findings in HBV-infected cells, for HCV infection, a study has reported that OPN-overexpressing Huh7 cells significantly increased HCV replication by suppressing IFN α stimulated genes (ISGs) via the inhibition of STAT-1 phosphorylation and degradation. (55) Moreover, the modulation of OPN levels by overexpressing or silencing OPN increased HCV and HIV replication in Huh 7.5 cells or primary macrophages, respectively. (56, 57) Importantly, a study has reported that OPN drives HBV replication and HBV-driven fibrogenesis. (58) However, these studies provided no link between enhanced liver stiffness and upregulation of HCV-HIV markers. Interestingly, our previous studies demonstrated an increased HCV-HIV mRNA expression and apoptosis induction in hepatocytes plated on fibrotic stiffness. (26) While hepatocyte apoptosis has been shown to induce pro-fibrotic activation of HSC in these infections (59–61), HBV infection seems to have different properties since we observed no increased apoptosis in cells transfected with HBV. At that point, we were not able to identify the mechanisms of increased viral infectivity in hepatocytes under fibrotic conditions and to link an increased liver stiffness to OPN upregulation and suppression of

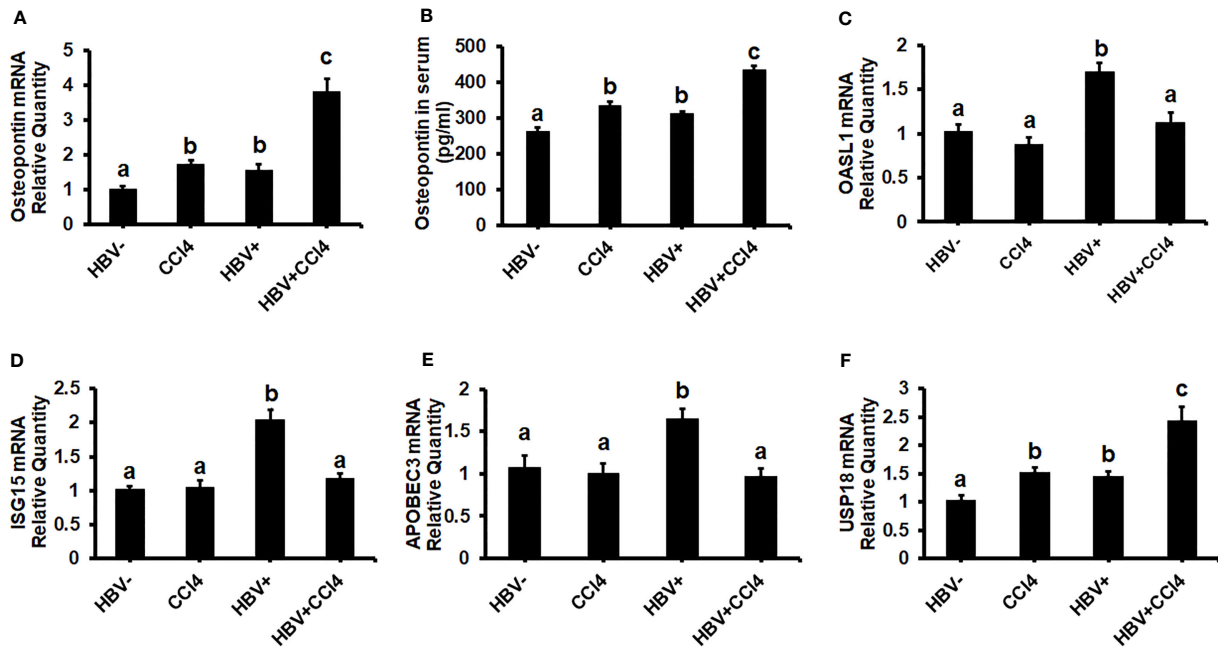


FIGURE 6
 Increased liver tissue stiffness promotes osteopontin which suppresses Interferon-Stimulated Gene (ISG) expression in the livers of CCl4-administered HBVTg mice: Liver fibrosis was induced by injecting CCl4 for 6 weeks in C57Bl/6 parental and HBV+ transgenic (HBVTg) mice. RT-PCR analysis was done for mRNA expression of OPN, IFN-induced genes, and USP18. (A) Osteopontin (OPN); (C) 2'-5' oligoadenylate synthetase-like 1 (OASL1); (D) Interferon-stimulated gene 15 (ISG15); (E) Apolipoprotein B Editing Complex (APOBEC3); (F) USP18. (B) OPN protein levels were measured by Elisa in serum. Data are expressed as Mean ± SEM (n = 4). The data bars marked with the same alphabetical letter are considered not significantly different, while those marked with differing alphabetical letters are considered significantly different from each other (p ≤ 0.05).

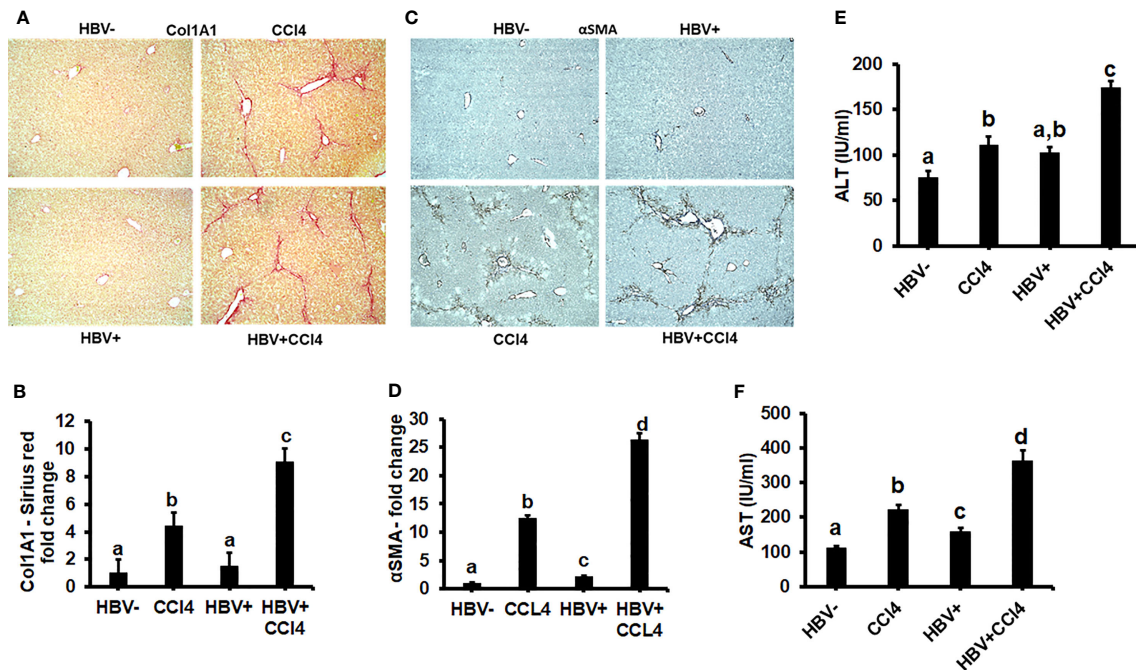


FIGURE 7
 CCl4 induces hepatic fibrosis in HBV- and HBV+ transgenic mice: Liver fibrosis was induced by injecting CCl4 for 6 weeks in C57Bl/6 parental and HBV+ transgenic (HBVTg) mice. (A, B) Collagen accumulation was visualized using sections of paraffin-embedded liver tissue which were subjected to picrosirius red staining; (C, D) α-Smooth muscle actin (α-SMA) protein levels were detected by immunohistochemical detection. Pictures were captured using a Keyence BZ-X810 fluorescence microscope. Staining intensity in the captured images was quantified using the Keyence BZ-X810 Analyzer software. At least 10 nonoverlapping fields per low magnification (20X) section were analyzed. (E, F) ALT and AST (serum enzymes) activities were determined in the serum of control and HBV-infected CCl4-administered mice. Data are expressed as Mean ± SEM (n = 4). The data bars marked with the same alphabetical letter are considered not significantly different, while those marked with differing alphabetical letters are considered significantly different from each other (p ≤ 0.05).

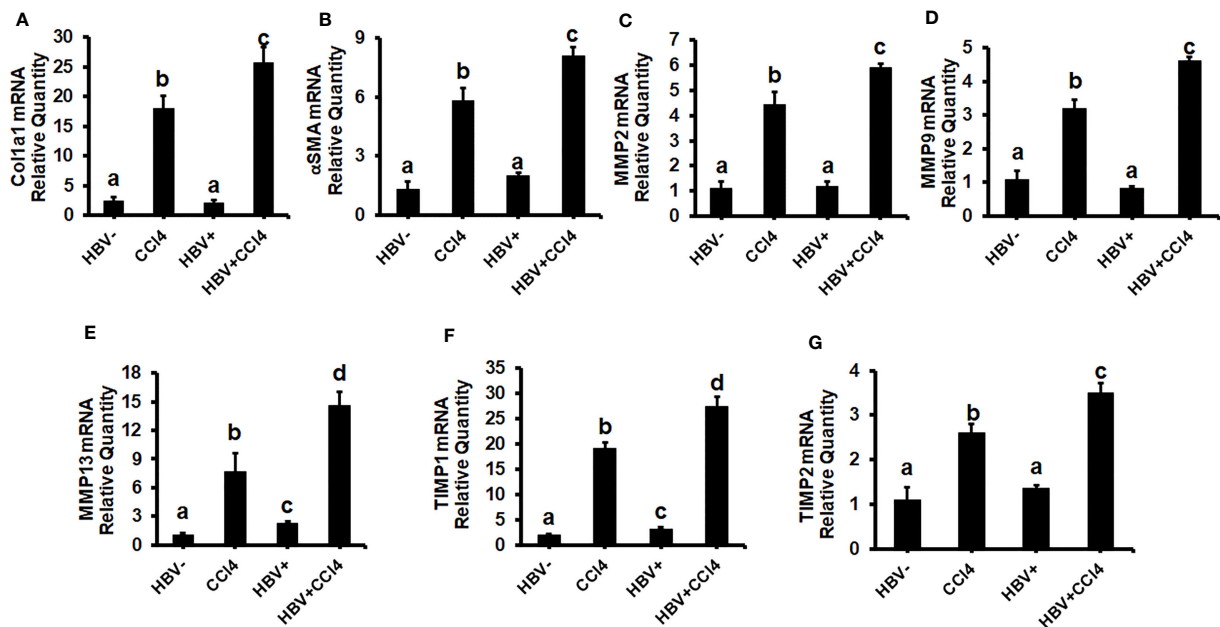


FIGURE 8

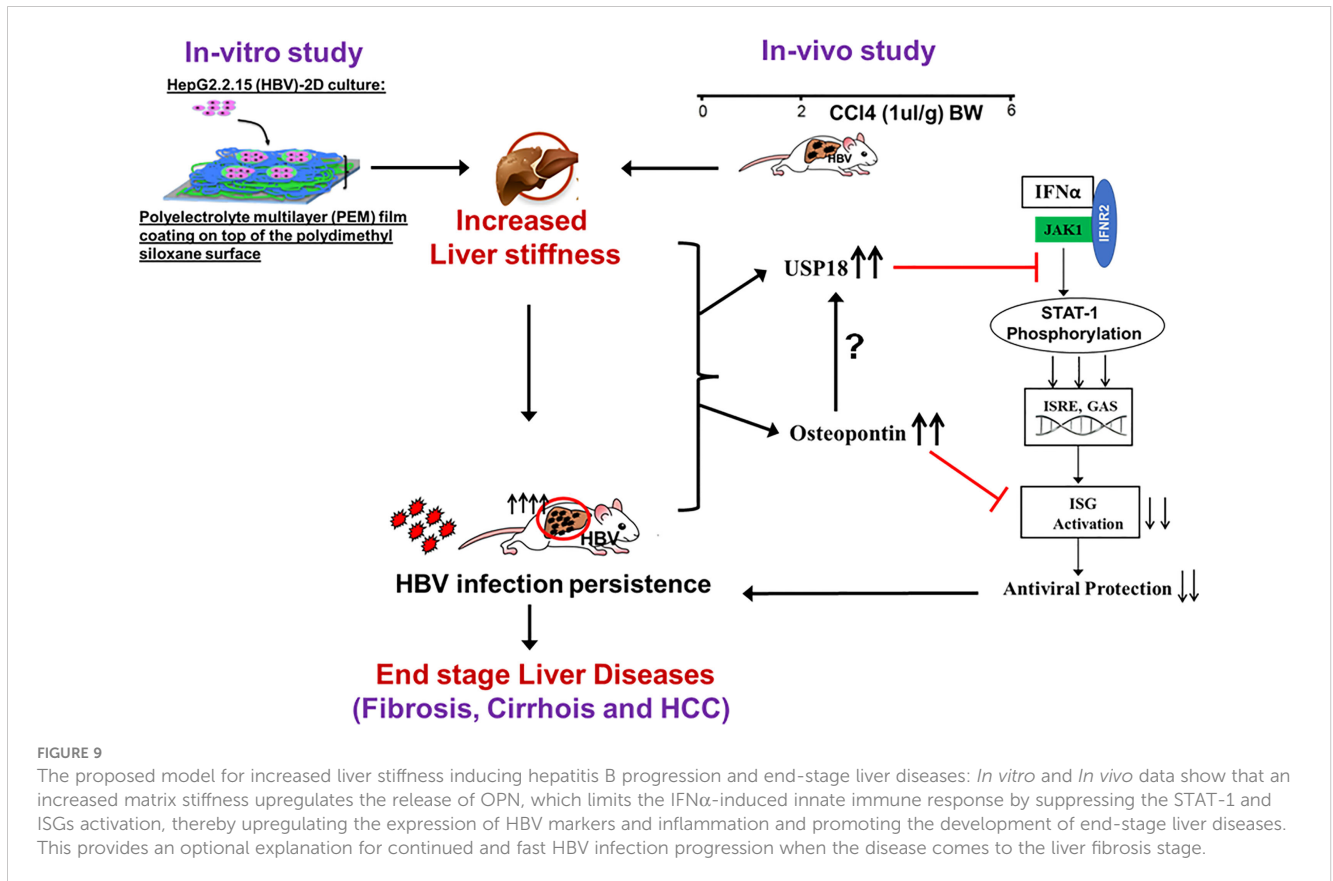
CCl4-administered HBV- and HBV+ transgenic mice show an increase in pro-fibrotic markers: Liver fibrosis was induced by injecting CCl4 for 6 weeks in C57Bl/6 parental and HBV+ transgenic (HBVTg) mice. RT-PCR analysis was done for mRNA expression of (A) Col1A1; (B) α-SMA; (C) MMP2; (D) MMP9; (E) MMP13; (F) TIMP1; and (G) TIMP2. Data are expressed as Mean ± SEM (n = 4). The data bars marked with the same alphabetical letter are considered not significantly different, while those marked with differing alphabetical letters are considered significantly different from each other (p ≤ 0.05).

innate immunity. However, in the current study, we observed a decrease in STAT-1 phosphorylation in stiff gel-attached HBV-transfected cells, and OPN overexpression suppressed ISGs, thereby increasing HBV RNA levels. As a next step, we investigated the relationship between OPN levels and USP18. We measured the *USP18* mRNA levels in rOPN-treated and OPN-silenced stiff gel-attached HBV-transfected cells (under fibrotic conditions). We found that only OPN-silenced cells show a decrease in *USP18* mRNA, while rOPN did not further increase the *USP18* mRNA levels. Interestingly, rOPN treatment significantly increased the *USP18* protein levels. This finding indicates that OPN partially contributes to the elevation of *USP18* and suggests that while OPN affects *USP18* expression, this protein is not a direct target for OPN and requires some intermediate “inserts”. Our *in vitro* study provides evidence that fibrotic stiffness induced OPN expression in hepatocytes, causing upregulation of HBV replication and HBV markers due to decreased innate immunity. In fact, it has been reported that in HBV infection, chronic liver inflammation coexists with impaired antiviral immunity though the exact mechanism has not been previously discovered (62).

As proof of concept that liver stiffness-induced OPN releases increased HBV replication, we conducted an *in vivo* experiment using C57Bl/6 parental (wild type) and HBV+ transgenic (HBVTg) mice. Although recent studies have shown the role of tissue stiffness in liver fibrogenesis, little is known about its role in HBV infection pathogenesis. This is the first *in vivo* study where we investigated the role of liver stiffness in HBV infection pathogenesis using HBVTg mice. To mimic fibrotic liver, hepatic fibrosis was established by administering CCl4 for 6 weeks. Here, we observed an enhanced liver stiffness and an upregulation of HBV-specific

markers with an increase in OPN expression in livers and serum of CCl4-administered HBVTg mice. Interestingly, the expression of IFN type 1-inducible anti-viral genes was decreased with an upregulation in *USP18* mRNA expression in fibrotic HBVTg mice. ALT and AST levels and fibrosis markers were higher in CCl4-administered HBVTg mice. The findings from this *in vivo* study were supported by our *in vitro* results as well as clinical studies by others, demonstrating that a high serum OPN level and high liver stiffness in chronic HBV infection predict the failure of virological response and hepatic fibrosis regression. (63) It has been reported that hepatic stiffness was important for monitoring the outcomes of hepatic fibrosis in HBV antiviral therapy, and long-term viral inhibition was correlated with the outcomes of hepatic fibrosis. (64) The present study provides valuable evidence on the importance of liver stiffness, OPN, and their relationship in the regulation of innate immunity in advanced HBV infection.

We cannot exclude that in the presence of macrophages and hepatic stellate cells, OPN release will be more potent and co-culture of hepatocytes with these cells would provide a more robust effect on hepatocyte infectivity. In fact, we observed it in our *in vivo* studies, where the magnitude of OPN response in the liver was higher than in hepatocyte monoculture. However, here, we tried to find an explanation for the up-regulation of HBV markers in infected hepatocytes plated on the stiff gel, and we believe that it is related to OPN-induced suppression of anti-viral ISGs. This has been demonstrated by overexpressing and knocking down OPN in HBV+ HepG2.2.15 cells. In future studies, we are planning to perform co-culture experiments for liver parenchymal and non-parenchymal cells or to look at their cell-to-cell interactions using liver organoids.



Based on our *in vitro* and *in vivo* data, we conclude that an increased matrix stiffness upregulates the release of OPN, which limits the IFN α -induced innate immune response by suppressing the STAT-1 and ISGs activation, thereby upregulating the expression of HBV markers and promoting the development of end-stage liver diseases (Figure 9). This provides an optional explanation for continued and fast HBV infection progression when the disease comes to the liver fibrosis stage.

Data availability statement

The original contributions presented in the study are included in the article/supplementary material. Further inquiries can be directed to the corresponding author.

Ethics statement

The animal study was reviewed and approved by Institutional Animal Care and Use Committee of University of Nebraska Medical Center.

Author contributions

MG, GB, YM, and WW: conducted experiments and evaluated data; SK: provided materials for the experiment and carried out the liver tissue stiffness measurement; MG and SK: interpreted results

and information obtained from experiments; KK, LP, and NO: edited the manuscript, provided suggestions to improve the project, and performed corrections; MG: obtained grant funding, developed and designed research project goals and experiments, and performed the final edit of the manuscript. All authors contributed to the article and approved the submitted version.

Funding

Funding for this work was obtained from the K01-Mentored Research Scientist Development Award- 1K01AA026864 provided by the National Institute on Alcohol Abuse and Alcoholism (NIAAA), USA, and the Nebraska Research Initiative (NRI) and Collaboration Initiative Grants, University of Nebraska NRI.

Acknowledgments

The authors would like to thank Dr. Jing-Hsiung James Ou, University of Southern California, Los Angeles, for providing HBV transgenic mice for breeding.

Conflict of interest

The authors declare that the research was conducted in the absence of any commercial or financial relationships that could be construed as a potential conflict of interest.

Publisher's note

All claims expressed in this article are solely those of the authors and do not necessarily represent those of their affiliated

organizations, or those of the publisher, the editors and the reviewers. Any product that may be evaluated in this article, or claim that may be made by its manufacturer, is not guaranteed or endorsed by the publisher.

References

- El-Serag HB. Epidemiology of viral hepatitis and hepatocellular carcinoma. *Gastroenterology* (2012) 142:1264–1273 e1261. doi: 10.1053/j.gastro.2011.12.061
- Locarnini S, Hatzakis A, Chen DS, Lok A. Strategies to control hepatitis B: Public policy, epidemiology, vaccine and drugs. *J Hepatol* (2015) 62:S76–86. doi: 10.1016/j.jhep.2015.01.018
- Lim CJ, Lee YH, Pan L, Lai L, Chua C, Wasser M, et al. Multidimensional analyses reveal distinct immune microenvironment in hepatitis B virus-related hepatocellular carcinoma. *Gut* (2019) 68:916–27. doi: 10.1136/gutjnl-2018-316510
- Revill PA, Chisari FV, Block JM, Dandri M, Gehring AJ, Guo H, et al. A global scientific strategy to cure hepatitis B. *Lancet Gastroenterol Hepatol* (2019) 4:545–58. doi: 10.1016/S2468-1253(19)30119-0
- Iannacone M, Guidotti LG. Immunobiology and pathogenesis of hepatitis B virus infection. *Nat Rev Immunol* (2022) 22:19–32. doi: 10.1038/s41577-021-00549-4
- Childs L, Roessel S, Tohme RA. Status and progress of hepatitis B control through vaccination in the South-East Asia Region 1992–2015. *Vaccine* (2018) 36:6–14. doi: 10.1016/j.vaccine.2017.11.027
- Shin EC, Sung PS, Park SH. Immune responses and immunopathology in acute and chronic viral hepatitis. *Nat Rev Immunol* (2016) 16:509–23. doi: 10.1038/nri.2016.69
- Tang CM, Yau TO, Yu J. Management of chronic hepatitis B infection: current treatment guidelines, challenges, and new developments. *World J Gastroenterol* (2014) 20:6262–78. doi: 10.3748/wjg.v20.i20.6262
- Inoue T, Tanaka Y. Novel biomarkers for the management of chronic hepatitis B. *Clin Mol Hepatol* (2020) 26:261–79. doi: 10.3350/cmh.2020.0032
- Leverro M, Zucman-Rossi J. Mechanisms of HBV-induced hepatocellular carcinoma. *J Hepatol* (2016) 64:S84–S101. doi: 10.1016/j.jhep.2016.02.021
- Mcmahon BJ. The natural history of chronic hepatitis B virus infection. *Hepatology* (2009) 49:S45–55. doi: 10.1002/hep.22898
- Parikh P, Ryan JD, Tsochatzis EA. Fibrosis assessment in patients with chronic hepatitis B virus (HBV) infection. *Ann Transl Med* (2017) 5:40. doi: 10.21037/atm.2017.01.28
- Georges PC, Hui JJ, Gombos Z, McCormick ME, Wang AY, Uemura M, et al. Increased stiffness of the rat liver precedes matrix deposition: implications for fibrosis. *Am J Physiol Gastrointest Liver Physiol* (2007) 293:G1147–1154. doi: 10.1152/ajpgi.00032.2007
- Masuzaki R, Tateishi R, Yoshida H, Yoshida H, Sato S, Kato N, et al. Risk assessment of hepatocellular carcinoma in chronic hepatitis C patients by transient elastography. *J Clin Gastroenterol* (2008) 42:839–43. doi: 10.1097/MCG.0b013e318050074f
- Liu L, Nie Y, Zhang Y, Liu Q, Zhu X. Liver Stiffness Is a Predictor of Rebleeding in Patients With Hepatitis B-Related Cirrhosis: A Real-World Cohort Study. *Front Med (Lausanne)* (2021) 8:690825. doi: 10.3389/fmed.2021.690825
- Tschumperlin DJ, Ligresti G, Hilscher MB, Shah VH. Mechanosensing and fibrosis. *J Clin Invest* (2018) 128:74–84. doi: 10.1172/JCI93561
- Lampi MC, Reinhart-King CA. Targeting extracellular matrix stiffness to attenuate disease: From molecular mechanisms to clinical trials. *Sci Transl Med* (2018) 10:ea00475. doi: 10.1126/scitranslmed.a00475
- Honsawek S, Chayanupatkul M, Chongsrisawat V, Vejchapipat P, Poorawan Y. Increased osteopontin and liver stiffness measurement by transient elastography in biliary atresia. *World J Gastroenterol* (2010) 16:5467–73. doi: 10.3748/wjg.v16.i43.5467
- You Y, Zheng Q, Dong Y, Wang Y, Zhang L, Xue T, et al. Higher Matrix Stiffness Upregulates Osteopontin Expression in Hepatocellular Carcinoma Cells Mediated by Integrin beta1/GSK3beta/Catenin Pathway. *PLoS One* (2015) 10:e0134243. doi: 10.1371/journal.pone.0134243
- Wen Y, Jeong S, Xia Q, Kong X. Role of Osteopontin in Liver Diseases. *Int J Biol Sci* (2016) 12:1121–8. doi: 10.7150/ijbs.16445
- Liu HB, Chen QY, Wang XY, Zhang LJ, Hu LP, Harrison TJ, et al. Infection with Hepatitis B Virus May Increase the Serum Concentrations of Osteopontin. *Intervirology* (2021) 64:126–34. doi: 10.1159/000513687
- Ramaiah SK, Rittling S. Pathophysiological role of osteopontin in hepatic inflammation, toxicity, and cancer. *Toxicol Sci* (2008) 103:4–13. doi: 10.1093/toxsci/kfn246
- Syn WK, Choi SS, Liaskou E, Karaca GF, Agboola KM, Oo YH, et al. Osteopontin is induced by hedgehog pathway activation and promotes fibrosis progression in nonalcoholic steatohepatitis. *Hepatology* (2011) 53:106–15. doi: 10.1002/hep.23998
- Morales-Ibanez O, Dominguez M, Ki SH, Marcos M, Chaves JF, Nguyen-Khac E, et al. Human and experimental evidence supporting a role for osteopontin in alcoholic hepatitis. *Hepatology* (2013) 58:1742–56. doi: 10.1002/hep.26521
- Natarajan V, Berglund EJ, Chen DX, Kidambi S. Substrate stiffness regulates primary hepatocyte functions. *RSC Adv* (2015) 5:80956–66. doi: 10.1039/C5RA15208A
- Ganesan M, Dagur RS, Makarov E, Poluektova LI, Kidambi S, Osna NA. Matrix stiffness regulate apoptotic cell death in HIV-HCV co-infected hepatocytes: Importance for liver fibrosis progression. *Biochem Biophys Res Commun* (2018) 500:717–22. doi: 10.1016/j.bbrc.2018.04.142
- Kidambi S. Stiffness and Hepatocytes Function *In Vitro*. In book: *Liver Elastography* (2020), 645–60. doi: 10.1007/978-3-030-40542-7_55
- Natarajan V, Moeller M, Casey CC, Harris EN, Kidambi S. Matrix Stiffness Regulates Liver Sinusoidal Endothelial Cell Function Mimicking Responses in Fatty Liver Disease. *bioRxiv*. (2020). doi: 10.1101/2020.01.27.921353
- Natarajan V, Moeun Y, Kidambi S. Exploring Interactions between Primary Hepatocytes and Non-Parenchymal Cells on Physiological and Pathological Liver Stiffness. *Biol (Basel)* (2021) 10:408. doi: 10.3390/biology10050408
- Zhao R, Wang TZ, Kong D, Zhang L, Meng HX, Jiang Y, et al. Hepatoma cell line HepG2.2.15 demonstrates distinct biological features compared with parental HepG2. *World J Gastroenterol* (2011) 17:1152–9. doi: 10.3748/wjg.v17.i9.1152
- Ganesan M, Krutik VM, Makarov E, Mathews S, Kharbanda KK, Poluektova LY, et al. Acetaldehyde suppresses the display of HBV-MHC class I complexes on HBV-expressing hepatocytes. *Am J Physiol Gastrointest Liver Physiol* (2019) 317:G127–40. doi: 10.1152/ajpgi.00064.2019
- Ganesan M, Mathews S, Makarov E, Petrosyan A, Kharbanda KK, Kidambi S, et al. Acetaldehyde suppresses HBV-MHC class I complex presentation on hepatocytes via induction of ER stress and Golgi fragmentation. *Am J Physiol Gastrointest Liver Physiol* (2020) 319:G432–42. doi: 10.1152/ajpgi.00109.2020
- Ganesan M, Wang W, Mathews S, Makarov E, New-Aaron M, Dagur RS, et al. Ethanol attenuates presentation of cytotoxic T-lymphocyte epitopes on hepatocytes of HBV-infected humanized mice. *Alcohol Clin Exp Res* (2022) 46:40–51. doi: 10.1111/acer.14740
- Constandinou Cc HN, Iredale J. Modeling liver fibrosis in rodents. In: Varga J, Brenner DA, Phan SH, editors. *Fibrosis Research: Methods and Protocols*. Totowa, NJ: Humana Press (2005). p. 237–50.
- Bennett RG, Heimann DG, Singh S, Simpson RL, Tuma DJ. Relaxin decreases the severity of established hepatic fibrosis in mice. *Liver Int* (2014) 34:416–26. doi: 10.1111/liv.12247
- Junqueira LC, Bignolas G, Brentani RR. Picrosirius staining plus polarization microscopy, a specific method for collagen detection in tissue sections. *Histochem J* (1979) 11:447–55. doi: 10.1007/BF01002772
- Weickenmeier J, Kurt M, Ozkaya E, De Rooij R, Ovaert TC, Ehman RL, et al. Brain stiffens post mortem. *J Mech Behav BioMed Mater* (2018) 84:88–98. doi: 10.1016/j.jmbm.2018.04.009
- Gehring AJ, Protzer U. Targeting Innate and Adaptive Immune Responses to Cure Chronic HBV Infection. *Gastroenterology* (2019) 156:325–37. doi: 10.1053/j.gastro.2018.10.032
- Megahed F, Zhou X, Sun P. The Interactions between HBV and the Innate Immunity of Hepatocytes. *Viruses* (2020) 12:285. doi: 10.3390/v12030285
- Xu C, Chen J, Chen X. Host Innate Immunity Against Hepatitis Viruses and Viral Immune Evasion. *Front Microbiol* (2021) 12:740464. doi: 10.3389/fmicb.2021.740464
- Lester SN, Li K. Toll-like receptors in antiviral innate immunity. *J Mol Biol* (2014) 426:1246–64. doi: 10.1016/j.jmb.2013.11.024
- Streicher F, Jouvenet N. Stimulation of Innate Immunity by Host and Viral RNAs. *Trends Immunol* (2019) 40:1134–48. doi: 10.1016/j.it.2019.10.009
- Gao B. Basic liver immunology. *Cell Mol Immunol* (2016) 13:265–6. doi: 10.1038/cmi.2016.09
- Ringelhan M, Pfister D, O'connor T, Pikarsky E, Heikenwalder M. The immunology of hepatocellular carcinoma. *Nat Immunol* (2018) 19:222–32. doi: 10.1038/s41590-018-0044-z
- Gao B, Jeong WI, Tian Z. Liver: An organ with predominant innate immunity. *Hepatology* (2008) 47:729–36. doi: 10.1002/hep.22034

46. Gao B, Seki E, Brenner DA, Friedman S, Cohen JI, Nagy L, et al. Innate immunity in alcoholic liver disease. *Am J Physiol Gastrointest Liver Physiol* (2011) 300:G516–525. doi: 10.1152/ajpgi.00537.2010
47. Reherrmann B. Pathogenesis of chronic viral hepatitis: differential roles of T cells and NK cells. *Nat Med* (2013) 19:859–68. doi: 10.1038/nm.3251
48. Peeridogah H, Meshkat Z, Habibzadeh S, Arzanlou M, Shahi JM, Rostami S, et al. Current concepts on immunopathogenesis of hepatitis B virus infection. *Virus Res* (2018) 245:29–43. doi: 10.1016/j.virusres.2017.12.007
49. Reherrmann B, Thimme R. Insights From Antiviral Therapy Into Immune Responses to Hepatitis B and C Virus Infection. *Gastroenterology* (2019) 156:369–83. doi: 10.1053/j.gastro.2018.08.061
50. Branchi F, Conti CB, Baccarin A, Lampertico P, Conte D, Fraquelli M. Non-invasive assessment of liver fibrosis in chronic hepatitis B. *World J Gastroenterol* (2014) 20:14568–80. doi: 10.3748/wjg.v20.i40.14568
51. Oliveri F, Coco B, Ciccorossi P, Colombatto P, Romagnoli V, Cherubini B, et al. Liver stiffness in the hepatitis B virus carrier: a non-invasive marker of liver disease influenced by the pattern of transaminases. *World J Gastroenterol* (2008) 14:6154–62. doi: 10.3748/wjg.14.6154
52. Kavak S, Kaya S, Senol A, Sogutcu N. Evaluation of liver fibrosis in chronic hepatitis B patients with 2D shear wave elastography with propagation map guidance: a single-centre study. *BMC Med Imaging* (2022) 22:50. doi: 10.1186/s12880-022-00777-7
53. Diao H, Liu X, Wu Z, Kang L, Cui G, Morimoto J, et al. Osteopontin regulates interleukin-17 production in hepatitis. *Cytokine* (2012) 60:129–37. doi: 10.1016/j.cyto.2012.06.287
54. Zhao L, Li T, Wang Y, Pan Y, Ning H, Hui X, et al. Elevated plasma osteopontin level is predictive of cirrhosis in patients with hepatitis B infection. *Int J Clin Pract* (2008) 62:1056–62. doi: 10.1111/j.1742-1241.2007.01368.x
55. Shirasaki T, Honda M, Yamashita T, Nio K, Shimakami T, Shimizu R, et al. The osteopontin-CD44 axis in hepatic cancer stem cells regulates IFN signaling and HCV replication. *Sci Rep* (2018) 8:13143. doi: 10.1038/s41598-018-31421-6
56. Brown A, Islam T, Adams R, Nerle S, Kamara M, Eger C, et al. Osteopontin enhances HIV replication and is increased in the brain and cerebrospinal fluid of HIV-infected individuals. *J Neurovirol* (2011) 17:382–92. doi: 10.1007/s13365-011-0035-4
57. Iqbal J, Sarkar-Dutta M, Mcrae S, Ramachandran A, Kumar B, Waris G. Osteopontin Regulates Hepatitis C Virus (HCV) Replication and Assembly by Interacting with HCV Proteins and Lipid Droplets and by Binding to Receptors alphaVbeta3 and CD44. *J Virol* (2018) 92:e02116–17. doi: 10.1128/JVI.02116-17
58. Phillips S, Mistry S, Coombes J, Hadzhiolova T, Doornebal E, Harris N, et al. Osteopontin drives HBV replication and HBV-driven fibrogenesis and represents a novel therapeutic target to achieve functional cure in chronic hepatitis B. *J Hepatol* (2020) 73:S845. doi: 10.1016/S0168-8278(20)32133-4
59. Ganesan M, Poluektova LY, Enweluzo C, Kharbanda KK, Osna NA. Hepatitis C Virus-Infected Apoptotic Hepatocytes Program Macrophages and Hepatic Stellate Cells for Liver Inflammation and Fibrosis Development: Role of Ethanol as a Second Hit. *Biomolecules* (2018) 8:113. doi: 10.3390/biom8040113
60. Ganesan M, New-Aaron M, Dagur RS, Makarov E, Wang W, Kharbanda KK, et al. Alcohol Metabolism Potentiates HIV-Induced Hepatotoxicity: Contribution to End-Stage Liver Disease. *Biomolecules* (2019) 9:851. doi: 10.3390/biom9120851
61. New-Aaron M, Dagur RS, Koganti SS, Ganesan M, Wang W, Makarov E, et al. Alcohol and HIV-Derived Hepatocyte Apoptotic Bodies Induce Hepatic Stellate Cell Activation. *Biol (Basel)* (2022) 11:1059. doi: 10.3390/biology11071059
62. Song H, Tan G, Yang Y, Cui A, Li H, Li T, et al. Hepatitis B Virus-Induced Imbalance of Inflammatory and Antiviral Signaling by Differential Phosphorylation of STAT1 in Human Monocytes. *J Immunol* (2019) 202:2266–75. doi: 10.4049/jimmunol.1800848
63. Osman H, Ghweil A, Khodeary A. Role of Plasma Osteopontin Level as a Predictor of Hepatic Fibrosis Regression and Response to Antiviral Treatment in Patients with Chronic HBV or Chronic HCV Infection. *Open J Gastroenterol* (2018) 8:434–47. doi: 10.4236/ojgas.2018.812045
64. Wu SD, Liu LL, Cheng JL, Liu Y, Cheng LS, Wang SQ, et al. Longitudinal monitoring of liver fibrosis status by transient elastography in chronic hepatitis B patients during long-term entecavir treatment. *Clin Exp Med* (2018) 18:433–43. doi: 10.1007/s10238-018-0501-x